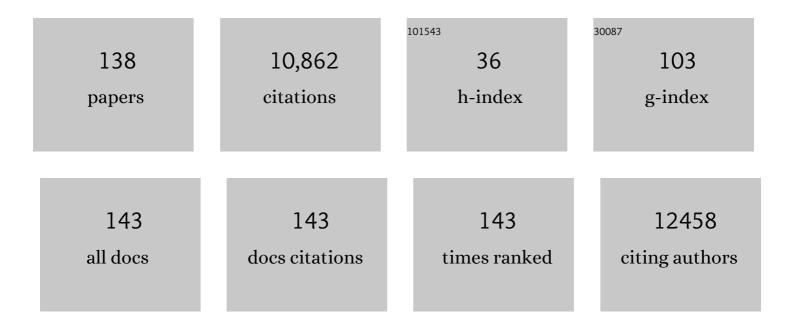
List of Publications by Year in descending order

Source: https://exaly.com/author-pdf/2130911/publications.pdf Version: 2024-02-01



#	Article	IF	CITATIONS
1	A homochiral metal–organic porous material for enantioselective separation and catalysis. Nature, 2000, 404, 982-986.	27.8	3,805
2	Wafer-Scale Growth of Single-Crystal Monolayer Graphene on Reusable Hydrogen-Terminated Germanium. Science, 2014, 344, 286-289.	12.6	831
3	Large-Scale Hierarchical Organization of Nanowire Arrays for Integrated Nanosystems. Nano Letters, 2003, 3, 1255-1259.	9.1	813
4	Molecular Container Assembly Capable of Controlling Binding and Release of Its Guest Molecules:Â Reversible Encapsulation of Organic Molecules in Sodium Ion Complexed Cucurbituril. Journal of the American Chemical Society, 1996, 118, 9790-9791.	13.7	342
5	Scalable Interconnection and Integration of Nanowire Devices without Registration. Nano Letters, 2004, 4, 915-919.	9.1	337
6	Polycatenated Two-Dimensional Polyrotaxane Net. Journal of the American Chemical Society, 1997, 119, 451-452.	13.7	291
7	Non-enzymatic electrochemical CuO nanoflowers sensor for hydrogen peroxide detection. Talanta, 2010, 80, 1648-1652.	5.5	280
8	Self-Assembly of a Polyrotaxane Containing a Cyclic "Bead―in Every Structural Unit in the Solid State:Â Cucurbituril Molecules Threaded on a One-Dimensional Coordination Polymer. Journal of the American Chemical Society, 1996, 118, 11333-11334.	13.7	228
9	Molecular Necklace:Â Quantitative Self-Assembly of a Cyclic Oligorotaxane from Nine Molecules. Journal of the American Chemical Society, 1998, 120, 4899-4900.	13.7	213
10	A Molecular Bowl with Metal Ion as Bottom: Reversible Inclusion of Organic Molecules in Cesium Ion Complexed Cucurbituril. Angewandte Chemie - International Edition, 1998, 37, 78-80.	13.8	204
11	Designed Self-Assembly of Molecular Necklaces. Journal of the American Chemical Society, 2002, 124, 2140-2147.	13.7	201
12	A Two-Dimensional Polyrotaxane with Large Cavities and Channels: A Novel Approach to Metal-Organic Open-Frameworks by Using Supramolecular Building Blocks. Angewandte Chemie - International Edition, 2001, 40, 399-402.	13.8	195
13	Large Thermoelectric Figure-of-Merits from SiGe Nanowires by Simultaneously Measuring Electrical and Thermal Transport Properties. Nano Letters, 2012, 12, 2918-2923.	9.1	181
14	Transition Metal Ion Directed Supramolecular Assembly of One- and Two-Dimensional Polyrotaxanes Incorporating Cucurbituril. Chemistry - A European Journal, 2002, 8, 498-508.	3.3	166
15	Nanolithography Using Hierarchically Assembled Nanowire Masks. Nano Letters, 2003, 3, 951-954.	9.1	151
16	Shape-Induced, Hexagonal, Open Frameworks: Rubidium Ion Complexed Cucurbituril. Angewandte Chemie - International Edition, 1999, 38, 641-643.	13.8	146
17	Stretchable, Transparent Zinc Oxide Thin Film Transistors. Advanced Functional Materials, 2010, 20, 3577-3582.	14.9	133
18	Helical polyrotaxane: cucurbituril â€~beads' threaded onto a helical one-dimensional coordination polymer. Chemical Communications, 1997, , 2361-2362.	4.1	117

#	Article	IF	CITATIONS
19	Columnar one-dimensional coordination polymer formed with a metal ion and a host–guest complex as building blocks: potassium ion complexed cucurbituril. Inorganica Chimica Acta, 2000, 297, 307-312.	2.4	102
20	Catalyst-free Growth of Single-Crystal Silicon and Germanium Nanowires. Nano Letters, 2009, 9, 864-869.	9.1	88
21	Layer-engineered large-area exfoliation of graphene. Science Advances, 2020, 6, .	10.3	81
22	Amperometric hydrogen peroxide biosensor based on a modified gold electrode with silver nanowires. Journal of Applied Electrochemistry, 2010, 40, 2099-2105.	2.9	76
23	Drastic improvement of oxide thermoelectric performance using thermal and plasma treatments of the InGaZnO thin films grown by sputtering. Acta Materialia, 2011, 59, 6743-6750.	7.9	66
24	Large-Scale Hierarchical Organization of Nanowires for Functional Nanosystems. Japanese Journal of Applied Physics, 2004, 43, 4465-4470.	1.5	65
25	A Simple Construction of a Rotaxane and Pseudorotaxane: Syntheses and X-Ray Crystal Structures of Cucurbituril Threaded on Substituted Spermine. Chemistry Letters, 1996, 25, 503-504.	1.3	64
26	Diameter-Controlled and Surface-Modified Sb2Se3 Nanowires and Their Photodetector Performance. Scientific Reports, 2014, 4, 6714.	3.3	59
27	Epitaxial Growth of a Single-Crystal Hybridized Boron Nitride and Graphene Layer on a Wide-Band Gap Semiconductor. Journal of the American Chemical Society, 2015, 137, 6897-6905.	13.7	55
28	A pseudo-capacitive chalcogenide-based electrode with dense 1-dimensional nanoarrays for enhanced energy density in asymmetric supercapacitors. Journal of Materials Chemistry A, 2016, 4, 10084-10090.	10.3	55
29	Graphene collage on Ni-rich layered oxide cathodes for advanced lithium-ion batteries. Nature Communications, 2021, 12, 2145.	12.8	54
30	Waferâ€Scale and Lowâ€Temperature Growth of 1Tâ€WS <sub>2</sub> Film for Efficient and Stable Hydrogen Evolution Reaction. Small, 2020, 16, e1905000.	10.0	53
31	Realization of continuous Zachariasen carbon monolayer. Science Advances, 2017, 3, e1601821.	10.3	46
32	Synthesis and characterization of a di-N-hydroxyethylated tetraaza macrocycle and its nickel(II) and copper(II) complexes: crystal structure of the nickel(II) complex. Journal of the Chemical Society Dalton Transactions, 1995, , 363.	1.1	45
33	Low-temperature wafer-scale growth of MoS2-graphene heterostructures. Applied Surface Science, 2019, 470, 129-134.	6.1	44
34	Guest-dependent [Cd(CN)2]nhost structures of cadmium cyanide–alcohol clathrates: two new [Cd(CN)2]nframeworks formed with PrnOH and PriOH guests. Journal of the Chemical Society Chemical Communications, 1993, , 1400-1402.	2.0	41
35	The influence of phonon scatterings on the thermal conductivity of SiGe nanowires. Applied Physics Letters, 2012, 101, 043114.	3.3	37
36	Pt-polyaniline nanocomposite on boron-doped diamond electrode for amperometic biosensor with low detection limit. Mikrochimica Acta, 2010, 171, 249-255.	5.0	36

#	Article	IF	CITATIONS
37	Seed-free electrochemical growth of ZnO nanotube arrays on single-layer graphene. Materials Letters, 2012, 72, 25-28.	2.6	33
38	Asymmetric induction in silyl nitronate cycloadditions to Oppolzer's chiral sultam derivatives. Tetrahedron: Asymmetry, 1991, 2, 27-30.	1.8	32
39	Entangled Germanium Nanowires and Graphite Nanofibers for the Anode of Lithium-Ion Batteries. Journal of the Electrochemical Society, 2013, 160, A112-A116.	2.9	31
40	Electrochemical growth of vertically aligned ZnO nanorod arrays on oxidized bi-layer graphene electrode. CrystEngComm, 2011, 13, 6036.	2.6	30
41	Deformation twinning of ultrahigh strength aluminum nanowire. Acta Materialia, 2018, 160, 14-21.	7.9	30
42	Ultrastable-Stealth Large Gold Nanoparticles with DNA Directed Biological Functionality. Langmuir, 2015, 31, 13773-13782.	3.5	29
43	Super-Nernstian pH Sensor Based on Anomalous Charge Transfer Doping of Defect-Engineered Graphene. Nano Letters, 2021, 21, 34-42.	9.1	29
44	Controlling electric potential to inhibit solid-electrolyte interphase formation on nanowire anodes for ultrafast lithium-ion batteries. Nature Communications, 2018, 9, 3461.	12.8	27
45	Toward Scalable Growth for Single-Crystal Graphene on Polycrystalline Metal Foil. ACS Nano, 2020, 14, 3141-3149.	14.6	26
46	Synthesis, characterization and crystal structures of novel hafnium porphyrins. Journal of the Chemical Society Dalton Transactions, 1993, , 205.	1.1	22
47	Self-Assembly of Interlocked Structures: Rotaxanes, Polyrotaxanes and Molecular Necklaces. Molecular Crystals and Liquid Crystals, 1999, 327, 65-70.	0.3	21
48	Graphene on Groupâ€IV Elementary Semiconductors: The Direct Growth Approach and Its Applications. Advanced Materials, 2019, 31, e1803469.	21.0	21
49	Amorphous germanium oxide nanobubbles for lithium-ion battery anode. Materials Research Bulletin, 2019, 110, 24-31.	5.2	21
50	Realization of Waferâ€Scale 1Tâ€MoS <sub>2</sub> Film for Efficient Hydrogen Evolution Reaction. ChemSusChem, 2021, 14, 1344-1350.	6.8	21
51	Analytical Characteristics of Electrochemical Biosensor Using Ptâ€Dispersed Graphene on Boron Doped Diamond Electrode. Electroanalysis, 2011, 23, 2408-2414.	2.9	20
52	Low-Programmable-Voltage Nonvolatile Memory Devices Based on Omega-shaped Gate Organic Ferroelectric P(VDF-TrFE) Field Effect Transistors Using p-type Silicon Nanowire Channels. Nano-Micro Letters, 2015, 7, 35-41.	27.0	20
53	Unraveling the Factors Affecting the Electrochemical Performance of MoS <sub>2</sub> –Carbon Composite Catalysts for Hydrogen Evolution Reaction: Surface Defect and Electrical Resistance of Carbon Supports. ACS Applied Materials & Interfaces, 2019, 11, 5037-5045.	8.0	20
54	Solution-Processed MoS <sub>2</sub> Film with Functional Interfaces via Precursor-Assisted Chemical Welding. ACS Applied Materials & amp; Interfaces, 2021, 13, 12221-12229.	8.0	19

#	Article	IF	CITATIONS
55	Crystal structures of (±)-1,2:4,5-di-O-isopropylidene-myoinositol and (±)-1,2:5,6-di-O-isopropylidene-myo-inositol: a conformational analysis. Carbohydrate Research, 1994, 253, 13-18.	2.3	18
56	Aromatic-aromatic ring interactions tested in cyclophanes. Bioorganic and Medicinal Chemistry Letters, 1993, 3, 263-268.	2.2	17
57	Tunable bandgap of a single layer graphene doped by the manganese oxide using the electrochemical doping. Applied Physics Letters, 2013, 102, 032106.	3.3	17
58	2D Doping Layer for Flexible Transparent Conducting Graphene Electrodes with Low Sheet Resistance and High Stability. Advanced Electronic Materials, 2018, 4, 1700622.	5.1	17
59	Selectivity of Threefold Symmetry in Epitaxial Alignment of Liquid Crystal Molecules on Macroscale Singleâ€Crystal Graphene. Advanced Materials, 2018, 30, e1802441.	21.0	17
60	Two new [Cd(CN)2]nframeworks with linear channels of large, elongated hexagonal cross-section: structures of cadmium cyanide–guest (guest = dmf and Me2SO) clathrates. Journal of the Chemical Society Chemical Communications, 1994, , 637-638.	2.0	16
61	Self-Assembly of Interlocked Structures and Open Framework Materials using Coordination Bonds. Molecular Crystals and Liquid Crystals, 2000, 342, 29-38.	0.3	16
62	Fabrication of one-dimensional devices by a combination of AC dielectrophoresis and electrochemical deposition. Nanotechnology, 2008, 19, 105305.	2.6	16
63	Catalytic etching of monolayer graphene at low temperature via carbon oxidation. Physical Chemistry Chemical Physics, 2016, 18, 101-109.	2.8	16
64	The catalytic activity of new ruthenium(II) complexes containing chelating diphosphine ligand in the homogeneous hydrogenation of cyclohexene. Polyhedron, 1994, 13, 1887-1894.	2.2	15
65	Microwave Characterization of a Single Wall Carbon Nanotube Bundle. Japanese Journal of Applied Physics, 2008, 47, 4965-4968.	1.5	15
66	Rational Design of Ultrathin Gas Barrier Layer via Reconstruction of Hexagonal Boron Nitride Nanoflakes to Enhance the Chemical Stability of Proton Exchange Membrane Fuel Cells. Small, 2019, 15, e1903705.	10.0	15
67	An Ecoâ€Friendly, CMOSâ€Compatible Transfer Process for Largeâ€Scale CVDâ€Graphene. Advanced Materials Interfaces, 2019, 6, 1900084.	3.7	15
68	Ultralow-power non-volatile memory cells based on P(VDF-TrFE) ferroelectric-gate CMOS silicon nanowire channel field-effect transistors. Nanoscale, 2015, 7, 11660-11666.	5.6	14
69	CMOS-compatible catalytic growth of graphene on a silicon dioxide substrate. Applied Physics Letters, 2016, 109, .	3.3	14
70	Defect-Free Mechanical Graphene Transfer Using <i>n-</i> Doping Adhesive Gel Buffer. ACS Nano, 2021, 15, 11276-11284.	14.6	14
71	Tunable threshold voltage of an n-type Si nanowire ferroelectric-gate field effect transistor for high-performance nonvolatile memory applications. Nanotechnology, 2014, 25, 205201.	2.6	13
72	Organic Electrolyte Based Pulsed Nanoplating and Fabrication of Carbon Nanotube Network Transistors. Japanese Journal of Applied Physics, 2011, 50, 06GE11.	1.5	13

#	Article	IF	CITATIONS
73	Silicon Embedded Nanoporous Carbon Composite for the Anode of Li Ion Batteries. Journal of the Electrochemical Society, 2012, 159, A1273-A1277.	2.9	12
74	Control of Lateral Dimension in Metal-Catalyzed Germanium Nanowire Growth: Usage of Carbon Sheath. Nano Letters, 2012, 12, 4007-4012.	9.1	12
75	Schottky Diode with Asymmetric Metal Contacts on WS <sub>2</sub> . Advanced Electronic Materials, 2022, 8, 2100941.	5.1	12
76	Fabrication of vertically aligned Si nanowires on Si (100) substrates utilizing metal-assisted etching. Journal of Vacuum Science and Technology A: Vacuum, Surfaces and Films, 2010, 28, 735-740.	2.1	11
77	A facile route to Si nanowire gate-all-around field effect transistors with a steep subthreshold slope. Nanoscale, 2013, 5, 8968.	5.6	11
78	Improved Contact Resistance by a Single Atomic Layer Tunneling Effect in WS 2 /MoTe 2 Heterostructures. Advanced Science, 2021, 8, 2100102.	11.2	11
79	Controlled growth of in-plane graphene/h-BN heterostructure on a single crystal Ge substrate. Applied Surface Science, 2021, 554, 149655.	6.1	11
80	Electrical Characteristics of the Backgated Bottom-Up Silicon Nanowire FETs. IEEE Nanotechnology Magazine, 2008, 7, 683-687.	2.0	10
81	Extracting Mobility Degradation and Total Series Resistance of Cylindrical Gate-All-Around Silicon Nanowire Field-Effect Transistors. IEEE Electron Device Letters, 2009, 30, 665-667.	3.9	10
82	Highly Efficient n-Type Doping of Graphene by Vacuum Annealed Amine-Rich Macromolecules. Materials, 2020, 13, 2166.	2.9	10
83	Twin boundary sliding in single crystalline Cu and Al nanowires. Acta Materialia, 2020, 196, 69-77.	7.9	10
84	Synthesis, characterization and structure of the highly sterically congested complex (3,14-dimethyl-14-nitromethyl-2,6,13,17-tetraazatricyclo[16.4.0.07.12]docos-2-ene)nickel diperchlorate and structure of (3,14-dimethyl-2,6,13,17-tetraazatricyclo[16.4.0.07.12]docosa-2,13-diene)nickel diperchlorate. Journal of the Chemical Society Dalton Transactions, 1994, , 853.	1.1	9
85	Microwave Characterization of a Field Effect Transistor with Dielectrophoretically-Aligned Single Silicon Nanowire. Japanese Journal of Applied Physics, 2010, 49, 06GG12.	1.5	9
86	Axial p–n Nanowire Gated Diodes as a Direct Probe of Surface-Dominated Charge Dynamics in Semiconductor Nanomaterials. Journal of Physical Chemistry C, 2011, 115, 23552-23557.	3.1	9
87	Core–shell Si <sub>1â^'x</sub> Ge <sub>x</sub> nanowires with controlled structural defects for phonon scattering enhancement. Journal of Materials Chemistry A, 2014, 2, 12153-12157.	10.3	9
88	Reliability Enhancement of Germanium Nanowires Using Graphene as a Protective Layer: Aspect of Thermal Stability. ACS Applied Materials & Interfaces, 2014, 6, 5069-5074.	8.0	9
89	Homogeneous hydrogenation with new cationic ruthenium(II) complexes of [RuH(CO)(NCCH3)(PPh3)2(diphos)]+ and [RuH(CO)(NCCH3)(PPh3)(diphos)]+. Crystal structure of [RuH(CO)(NCCH3)(PPh3) (Fe(î·5-C5H4PPh2)2)][BF4]. Polyhedron, 1996, 15, 3811-3820.	2.2	8
90	Electrical characteristics of nickel silicide–silicon heterojunction in suspended silicon nanowires. Solid-State Electronics, 2011, 56, 130-134.	1.4	8

#	Article	IF	CITATIONS
91	High performance Si nanowire field-effect-transistors based on a CMOS inverter with tunable threshold voltage. Nanoscale, 2014, 6, 5479.	5.6	8
92	Carbon out-diffusion mechanism for direct graphene growth on a silicon surface. Acta Materialia, 2015, 96, 18-23.	7.9	8
93	Loose-fit graphitic encapsulation of silicon nanowire for one-dimensional Si anode design. Journal of Materials Science and Technology, 2017, 33, 1120-1127.	10.7	8
94	Amperometric Glucose Biosensor Based on a Pt-Dispersed Hierarchically Porous Electrode. Journal of the Korean Physical Society, 2009, 54, 1612-1618.	0.7	8
95	Control of selective and catalyst-free growth of Sb2Te3 and Te nanowires from sputter-deposited Al-Sb-Te thin films. CrystEngComm, 2012, 14, 4255.	2.6	7
96	Graphene/PVDF Composites for Ni-rich Oxide Cathodes toward High-Energy Density Li-ion Batteries. Materials, 2021, 14, 2271.	2.9	7
97	Catalyst-free growth of Sb2Te3 nanowires. Materials Letters, 2011, 65, 812-814.	2.6	6
98	Gate-dependent photoconductivity of single layer graphene grafted with metalloporphyrin molecules. Applied Physics Letters, 2012, 100, .	3.3	6
99	Ultralow power complementary inverter circuits using axially doped p- and n-channel Si nanowire field effect transistors. Nanoscale, 2016, 8, 12022-12028.	5.6	6
100	Growth of quantum dot coated core-shell anisotropic nanowires for improved thermal and electronic transport. Applied Physics Letters, 2019, 114, 243104.	3.3	6
101	Morphology of Ti on Monolayer Nanocrystalline Graphene and Its Unexpectedly Low Hydrogen Adsorption. Journal of Physical Chemistry C, 2019, 123, 1572-1578.	3.1	6
102	Electrical characteristics of Si-nanoparticle/Si-nanowire-based field-effect transistors. Journal of Materials Science, 2008, 43, 3424-3428.	3.7	5
103	Fabrication and Characterization of Sidewall Defined Silicon-on-Insulator Single-Electron Transistor. IEEE Nanotechnology Magazine, 2008, 7, 544-550.	2.0	5
104	P-type silicon nanowire-based nano-floating gate memory with Au nanoparticles embedded in Al2O3 gate layers. Solid State Sciences, 2010, 12, 745-749.	3.2	5
105	Graphene arch gate SiO2 shell silicon nanowire core field effect transistors. Applied Physics Letters, 2011, 99, 212102.	3.3	5
106	Single inorganic-organic hybrid photovoltaic nanorod. Applied Physics Letters, 2013, 103, 143101.	3.3	5
107	Graphene shell on silica nanowires toward a nanostructured electrode with controlled morphology. Applied Physics Letters, 2013, 103, .	3.3	5
108	Large reduction in thermal conductivity for SiGe alloy nanowire wrapped with a Ge nanoparticle-embedded SiO <sub>2</sub> shell. Nanotechnology, 2016, 27, 305703.	2.6	5

#	Article	IF	CITATIONS
109	Template-Assisted CVD Growth of Silicon Nanowires on a Gram Scale. Journal of the Korean Physical Society, 2009, 54, 152-156.	0.7	5
110	The chemistry and catalytic activity of new cationic ruthenium(II) complexes in the hydrogenation of cyclohexene. Crystal structure of [RuH(CO)(PPh3)(P(OMe)3)(Ph2PCH2CH2AsPh2)]ClO4A·nâ^2C5H12. Polyhedron, 1996, 15, 1473-1479.	2.2	4
111	Metastable Ge <sub>1–<i>x</i></sub> C <sub><i>x</i></sub> Alloy Nanowires. ACS Applied Materials & Interfaces, 2012, 4, 805-810.	8.0	3
112	Thermoelectric Properties of Nanowires with a Graphitic Shell. ChemSusChem, 2015, 8, 2372-2377.	6.8	3
113	Elucidation of the role of lithium iodide as an additive for the <scp>liquidâ€based</scp> synthesis of <scp> Li <sub>7</sub> P <sub>2</sub> S <sub>8</sub> I </scp> solid electrolyte. International Journal of Energy Research, 2020, 44, 11542-11549.	4.5	3
114	A phase-convertible fast ionic conductor with a monolithic plastic crystalline host. Journal of Materials Chemistry A, 2021, 9, 10838-10845.	10.3	3
115	Performance Improvement of Residue-Free Graphene Field-Effect Transistor Using Au-Assisted Transfer Method. Sensors, 2021, 21, 7262.	3.8	3
116	GROWTH OF HIGH QUALITY ZINC OXIDE NANOWIRES BY SIMPLE OXIDATION OF ZINC POWDER IN AIR. Nano, 2008, 03, 477-482.	1.0	2
117	Large-Scale Solution-Phase Growth of Cu-Doped ZnO Nanowire Networks. Journal of Nanoscience and Nanotechnology, 2011, 11, 6062-6066.	0.9	2
118	Physicsâ€based modeling and microwave characterization of graphene coâ€planar waveguides. Physica Status Solidi - Rapid Research Letters, 2014, 8, 617-620.	2.4	2
119	One-pot size-controlled growth of graphene-encapsulated germanium nanocrystals. Applied Surface Science, 2018, 440, 553-559.	6.1	2
120	Hydrogen Evolution Reaction: Waferâ€Scale and Lowâ€Temperature Growth of 1Tâ€WS <sub>2</sub> Film for Efficient and Stable Hydrogen Evolution Reaction (Small 6/2020). Small, 2020, 16, 2070033.	10.0	2
121	Self-Catalytic Growth of Elementary Semiconductor Nanowires with Controlled Morphology and Crystallographic Orientation. Nano Letters, 2021, 21, 9909-9915.	9.1	2
122	Synthesis of Small Diameter Silicon Nanowires on SiO2 and Si3N4 Surfaces. IEICE Transactions on Electronics, 2010, E93-C, 546-551.	0.6	1
123	Fabrication of graphene field-effect transistors by simple stripping from CVD-grown layers. , 2010, , .		1
124	Aluminum Nanotransmission Lines with No Grain Boundaries and No Surface Roughness. Applied Physics Express, 2011, 4, 064104.	2.4	1
125	Organic Electrolyte Based Pulsed Nanoplating and Fabrication of Carbon Nanotube Network Transistors. Japanese Journal of Applied Physics, 2011, 50, 06GE11.	1.5	1
126	Atomic-scale Investigation of Interface Between Graphene Monolayer and Ge(110). Journal of the Korean Physical Society, 2019, 74, 241-244.	0.7	1

#	Article	IF	CITATIONS
127	Methane-Mediated Vapor Transport Growth of Monolayer WSe2 Crystals. Nanomaterials, 2019, 9, 1642.	4.1	1
128	Millimeter-Scale Growth of Single-Oriented Graphene on a Palladium Silicide Amorphous Film. ACS Nano, 2019, 13, 1127-1135.	14.6	1
129	hBN Flake Embedded Al2O3 Thin Film for Flexible Moisture Barrier. Materials, 2021, 14, 7373.	2.9	1
130	Electrical characteristics of the back-gated bottom-up silicon nanowire field effect transistor. , 2008, , .		0
131	pH dependent electrical characteristic of bottom-up synthesized silicon nanowire FETs with DDT passivation. , 2009, , .		0
132	RF Characterization of Germanium Nanowire Field Effect Transistors. AIP Conference Proceedings, 2011, , .	0.4	0
133	Synthesized Aluminum Nanowires for Future Interconnects [Nanopackaging]. IEEE Nanotechnology Magazine, 2012, 6, 24-26.	1.3	0
134	Morphology Control of Self-Catalyzed Germanium Nanostructures with Graphitic Carbon Shell. Journal of Nanoscience and Nanotechnology, 2012, 12, 4103-4107.	0.9	0
135	Water-induced room-temperature transformation of straight Ge/Si core/shell nanowires into circular silica nanotubes. CrystEngComm, 2015, 17, 6142-6148.	2.6	0
136	Chemical Vapor Deposition: An Ecoâ€Friendly, CMOSâ€Compatible Transfer Process for Largeâ€Scale CVDâ€Graphene (Adv. Mater. Interfaces 13/2019). Advanced Materials Interfaces, 2019, 6, 1970087.	3.7	0
137	Deoxyribonucleic Acid Sensitive Graphene Field-Effect Transistors. IEICE Transactions on Electronics, 2011, E94-C, 826-829.	0.6	0
138	Crystal structures of (±)-1,4-di-O-benzoyl-2,3-O-isopropylidene-myo-inositol and (±)-1,4-di-O-benzoyl-5,6-O-isopropylidene-myo-inositol: a conformational analysis. Carbohydrate Research, 1996, 295, 1-6.	2.3	0